ELSEVIER

Journal of Molecular Catalysis A: Chemical 170 (2001) 155–163

JOURNAL OF MOLECULAR CATALYSIS A: CHEMICAL

www.elsevier.com/locate/molcata

Carbon nanofiber supported palladium catalyst for liquid-phase reactions An active and selective catalyst for hydrogenation of cinnamaldehyde into hydrocinnamaldehyde

Cuong Pham-Huu [a], Nicolas Keller [a], Gabrielle Ehret [c], Loïc J. Charbonniere [b], Raymond Ziessel [b], Marc J. Ledoux [a,*]

[a] *Sous-unité Chimie des Matériaux Catalytiques, Laboratoire des Matériaux, Surfaces et Procédés Pour la Catalyse (LMSPC), ECPM-ULP, UMR 7515 du CNRS, 25, rue Becquerel, 67087 Strasbourg Cedex 2, France*

[b] *Laboratoire de Chimie, d'Electronique et Photonique Moléculaires, ECPM-ULP, UPRES-A 7008 CNRS, 25, rue Becquerel, 67087 Strasbourg Cedex 2, France*

[c] *Groupe Surface & Interface, IPCMS-ULP, UMR 7504 CNRS, 23, rue du Loess, 67037 Strasbourg Cedex, France*

Accepted 24 January 2001

Abstract

Carbon nanofibers (CNFs) prepared by decomposition of ethane over a Ni/alumina catalyst, are used as support for palladium clusters. The carbon support displays a mean diameter of 40–50 nm, lengths up to several tens of micrometers, as highlighted by transmission electron microscopy (TEM) observations and a specific surface area of about 50 m^2/g. The spheroidal palladium particles have a relatively homogeneous and sharp size distribution, centered at around 4 nm. This novel Pd/carbon nanofiber catalyst displays unusual catalytic properties and is successfully used in the selective hydrogenation of the C=C bond in cinnamaldehyde at a reaction temperature of around 80°C, under continuous hydrogen flowing at atmospheric pressure. The high performances of this novel catalyst in terms of efficiency and selectivity are, respectively, related to the inhibition of the mass-transfer processes over this non-porous material and to peculiar palladium–carbon interactions. It is concluded that the absence of microporosity in the carbon nanofibers favours both the high activity and selectivity which is confirmed by comparison with the commercially available high surface area charcoal supported palladium catalyst.

Keywords: Palladium catalyst; Carbon nanofibers; High surface area; Cinnamaldehyde hydrogenation

1. Introduction

Since their discovery at the beginning of the last decade [1], carbon nanotubes and nanofibers have received an increasing interest both from a fundamental point of view and for potential industrial applications [2–11]. Such applications may include their use as magnetic or sensoring materials, for gas separation and storage, but the most promising seems to be as catalyst supports [12–14]. Such structures can display unusual behaviors compared to classical supports, especially for liquid-phase reactions, in

* Corresponding author. Tel.: +33-3-8813-68-81; fax: +33-3-8813-68-80.
E-mail address: ledoux@cournot.u-strasbg.fr (M.J. Ledoux).

1381-1169/01/$ – see front matter
PII: S1381-1169(01)00055-3

which diffusion of reactants into the solid matrix and back-diffusion of the products outside the support are significantly influenced by the external size of the particles [15–18]. Furthermore, grain-shaped catalysts can replace homogeneous catalysts, because of their advantages in terms of catalyst and product separation, catalyst recovery and reduction of waste water containing the catalyst. Nanofibers supported catalysts can exhibit the same properties. Finally, it is worth pointing out that the literature data on such materials, for liquid-phase reactions, has been relatively scarce up to now.

Geus et al. [19] have reported that carbon nanofibril material, after suitable treatment, can be a good candidate as a support carrier for Pd in liquid-phase media. However, a conventional catalyst supported on activated charcoal exhibits a catalytic activity for hydrogenation of nitrobenzene as high as that obtained on a carbon nanofibril-based catalyst, showing the weak influence of the solid support on the catalytic performance. On the other hand, Baker and co-workers [13,14] have reported that nickel decorating carbon nanofibers (CNFs) exhibits a high catalytic activity when compared to classical supported catalysts, for light hydrocarbon hydrogenation reactions in the gas-phase, at atmospheric pressure. It was suggested by the authors that when nickel is supported on graphite nanofibers, the metal crystallites adopt a different morphology, i.e. hexagonal thin morphology, compared to those observed when the nickel is dispersed on classical support carriers such as alumina or silica. Such a peculiar metal morphology observed on the carbon nanofiber carrier was considered to be due to a strong metal–support interaction between nickel crystallites and exposed graphite planes.

Additionally, the hydrogenation of α-, β-unsaturated aldehydes to give selectively saturated aldehydes or saturated alcohols, as well as unsaturated alcohols, could be achieved by choosing suitable metal complex catalysts [20–24]. Much interest has been focused on the use of water-soluble homogeneous catalysts, despite the critical drawbacks related to such catalysts. On the other hand, several studies have been devoted to the use of heterogeneous catalysts for the obtention of relatively selective C=O bond hydrogenation [25–29].

The aim of the present work is to report the preparation and the characterization of a palladium-decorated carbon nanofiber catalyst and its implication in hydrogenation reactions. The catalytic activity was investigated for the liquid-phase selective hydrogenation of cinnamaldehyde into the corresponding saturated aldehyde (hydrocinnamaldehyde) in mild reaction conditions, i.e. temperature = 100°C and atmospheric pressure of hydrogen. Comparison was made with a commercially available activated charcoal supported palladium catalyst in term of activity, expressed as conversion, and selectivity towards C=C and C=O bond hydrogenation. The microstructure of the support and of the catalyst was studied using high-resolution transmission electron microscopy, and its influence on catalytic performance is discussed.

2. Experimental

2.1. Carbon nanofibers

The CNF support was synthesized by catalytic hydrocarbon decomposition over a high surface area alumina supported nickel catalyst. The nickel catalyst was prepared by incipient wetness impregnation of the alumina support with an aqueous solution of nickel nitrate containing 20 vol.% of glycerol as a visqueous agent which allows the obtention of a highly dispersed metallic-phase [30]. The solid was dried in an oven at 200°C for 2 h in order to decompose the nitrate salt and the glycerol. The nickel loading measured by the inducted coupled plasma technique was 20 wt.%. The catalyst was reduced in situ under flowing hydrogen at 600°C for 0.5 h, and the reaction temperature was then increased from 600 to 750°C under a mixture of ethane and hydrogen (70:40 ml/min). After 12 h at this temperature, the reactor was cooled down to room temperature and the solid was discharged. The resulting solid was dispersed in a water:ethanol:*n*-hexane (1:1:1) mixture. Carbon nanofiber separation was performed by sonication and filtration (36 μm). The as-prepared carbon nanofibers were subsequently purified by acid treatment at 80°C for 2 h in order to dissolve the residual nickel catalyst which could be contained in their structure. The residual alumina was removed by concentrated soda treatment at 80°C for 4 h. The solid was filtered and washed several times with hot distilled water until the pH reached 7 and then dried overnight at 200°C.

2.2. Deposition mode

The palladium deposition (5 wt.%) was carried out by the incipient wetness impregnation technique with an aqueous solution containing the palladium nitrate salt. The wet solid was dried under vacuum at 60°C and the resulting dry solid was subsequently reduced under flowing hydrogen at 350°C for 2 h. The reactor was then cooled down under helium to room temperature and discharged without passivation. TEM characterization performed on the non-passivated and the passivated material with an oxygen flow (O_2 1 vol.% in helium) at room temperature showed no significant differences between the two samples. The reduced catalyst was stored under an argon atmosphere in order to avoid any surface oxidation of the palladium crystallites at room temperature.

2.3. Characterization techniques

The surface area and pore size measurement of the material were carried out on a Coulter SA-3100 porosimeter using N_2 as adsorbant at LN_2. Before the N_2 adsorption, the material was outgased at 200°C for 1 h in order to desorb impurities or moisture adsorbed from its surface.

The microstructure of the carbon nanofiber supported palladium material was observed by TEM (Topcon 200B working under 200 kV with a point-to-point resolution of 0.17 nm). The samples were prepared by grinding the catalysts following dispersion in ethanol and bringing the powder into contact with a holey carbon-coated copper grid. Great care was taken during the TEM experiments in order to avoid heating effects from the incident beam.

2.4. Selective hydrogenation of cinnamaldehyde

The hydrogenation of cinnamaldehyde was carried out at atmospheric pressure and low temperature, i.e. <100°C, in a microreactor. The solution contained 40 ml of dioxane, 0.260 g of reactant and the catalyst, corresponding to 1.05×10^{-3} g of Pd. Dioxane was used instead of alcohol in order to avoid any homogeneous reactions which could lead to the formation of heavier by-products [31–35]. Argon at room temperature bubbled through the liquid-phase which was stirred for 1 h in order to remove traces of dissolved oxygen in the medium, before introducing the catalyst and switching to the hydrogen flow. This hydrogen flow was continuously fed through the liquid-phase (10 cm^3/min), kept under vigorous stirring (500 rpm) for 1 h at room temperature before increasing the reaction temperature. The hydrogen stream was regulated by a Brooks 5850 TR mass flowmeter linked to a Brooks 5876 control unit. The cinnamaldehyde concentration and the product distribution were followed as a function of time on stream by gas chromatography analyses of microsamples periodically withdrawn and diluted with dioxane.

The analysis of the reaction products was performed on a Varian 3400-CX gas chromatograph (GC) equipped with a PONA capillary column coated with methyl siloxane (Hewlett-Packard, length 50 m, 0.2 mm i.d., film thickness 0.5 mm) and a flame ionization detector (FID). The products were calibrated by using pure components, i.e. cinnamaldehyde, cinnamyl alcohol, 3-phenylpropyl alcohol and 3-phenylpropionaldehyde (ACROS, purity > 98%) diluted in a dioxane solution. The analytical error calculated from the GC was within 2%. The conversion and product distribution were calculated from the GC analysis.

Cinnamaldehyde (ACROS) was used as received. GC analysis indicated a purity of 98.8%, the major organic impurities being cinnamyl alcohol (0.1%), 3-phenylpropyl alcohol (0.2%). H_2 (Air Liquide, grade U) was used as-received.

3. Results and discussion

3.1. Carbon nanofiber characterization

TEM micrographs of the starting carbon nanofibers are presented in Fig. 1. The low-magnification TEM micrograph (Fig. 1a) shows that the carbon nanofibers had a mean diameter centered at around 40–50 nm and lengths up to several tens of micrometers. Almost no traces of other carbon species (<10% from statistical TEM measurements) were detected on the sample, evidencing the high selectivity of the synthesis method. This contrasted with the presence in a significant amount up to several tens of percent of other forms of carbon, i.e. amorphous carbon and carbon nanoparticles, along with carbon nanofibers, observed

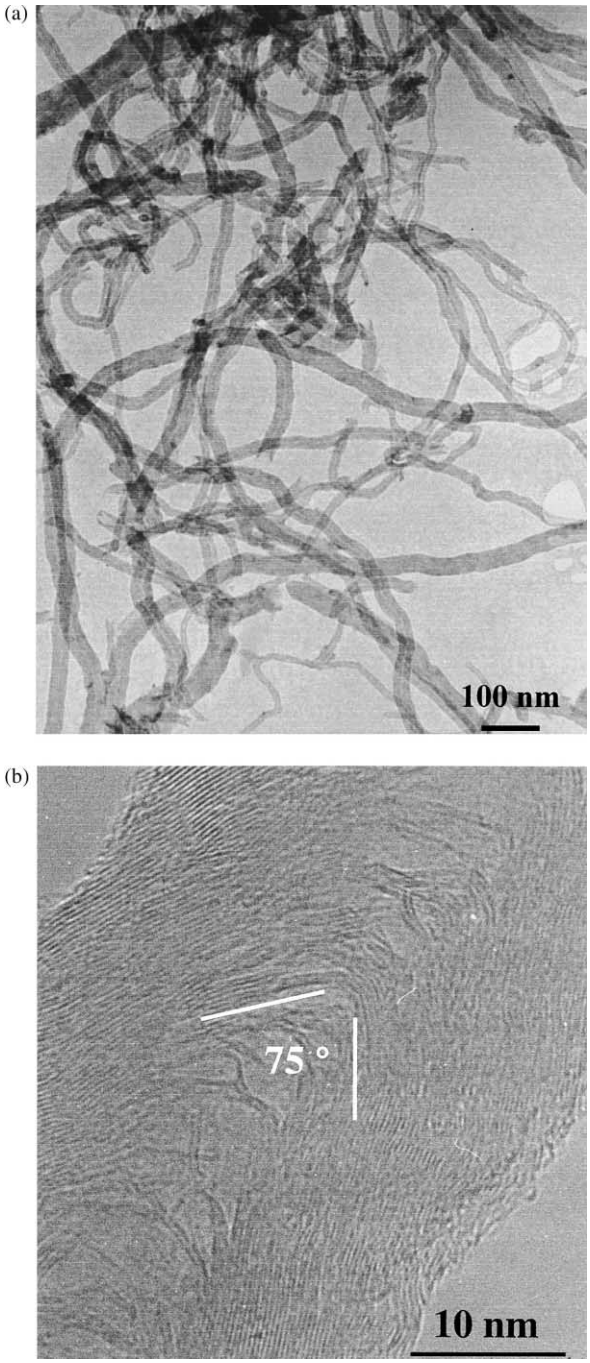

Fig. 1. (a) Transmission electron microscopy image of carbon nanofibers obtained by reaction at 750°C of an ethane/H_2 mixture on an alumina supported nickel catalyst; (b) high resolution TEM image of a carbon nanofiber.

for other methods of synthesis such as carbon-arc production or plasma decomposition [37–40]. One could note the absence of any nickel or alumina particles in the sample evidencing the high efficiency of the purification treatments.

The material consisted of graphite planes (separated by a distance of 0.32–0.34 nm) oriented at an angle of 75° in a fishbone stacking arrangement (Fig. 1b). This was consistent with the carbon nanostructures obtained over nickel-based catalysts reported by other authors [3,19,36]. The high-resolution TEM micrograph showed that the microstructure of the nanofibers was highly disorganized and only short crystalized periods were observed along the fiber axis.

The specific surface area of these carbon nanofibers was around 50 m^2/g with no microporosity. Such a surface area was relatively low compared to those reported in the literature for similar materials, i.e. >100 m^2/g [41]. This difference could be due to the synthesis parameters used for generation of the carbon nanostructured compounds, i.e. reaction temperature, nature of the gaseous reactants and catalysts. It has been recently reported by Teunissen [42] that depending on the synthesis conditions, significant differences were observed on the final carbon structure and the resulting properties. In some cases, the presence of amorphous carbon on the sample also induced an increase of the specific surface area.

3.2. Carbon nanofiber supported palladium

The HRTEM micrograph of the carbon nanofiber supported palladium material (Fig. 2) evidenced the high and homogeneous dispersion of spheroidal palladium metal particles on the outer surface of the carbon nanofibers, with a sharp particle size distribution centered at around 3–5 nm of diameter (Fig. 3). One could attribute this homogeneous dispersion to a relatively strong metal–support interaction between the metal salt precursor and the graphite edges of the carbon nanofibers, thus, increasing resistance to the growth of the palladium particles. It has been observed in our laboratory that the degree of dispersion of the metallic-phase was significantly modified depending on the carbon nanostructure conformations, i.e. nanotubes or nanofibers. Similar results have been reported by Kumbhar et al. during their work on carbon nanotube supported ruthenium [43]. The authors

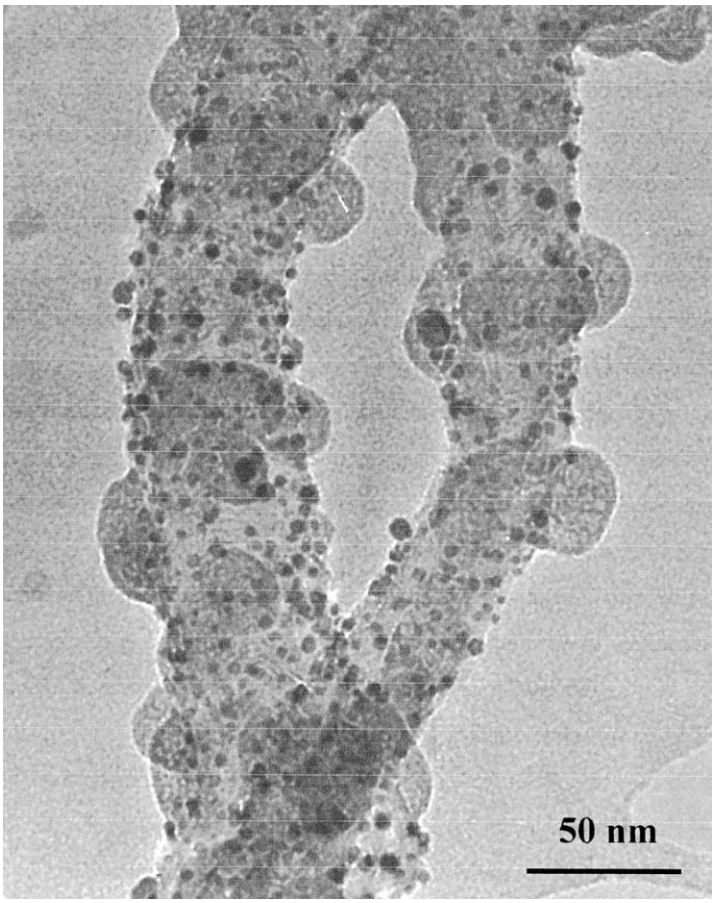

Fig. 2. TEM image of the carbon nanofiber supported palladium catalyst.

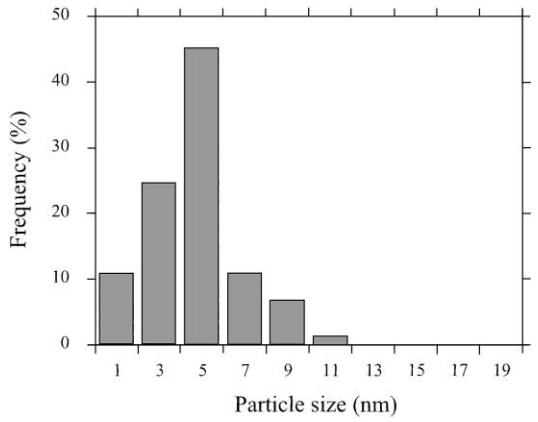

Fig. 3. Particle distribution in terms of diameter measured for 400 particles on a statistical sample of TEM micrographs.

showed by HRTEM: (i) the homogeneous distribution of metallic clusters on the nanotubes (particle range in diameter from 3 to 7 nm); and (ii) that ruthenium clusters were deposited on the external surface of the tubes.

A similar observation has also been reported by Baker and co-workers for a graphite nanofiber supported nickel catalyst [12–14]. However, the distribution profile of the particles deposited on graphite nanofibers was relatively broad, ranging in size from 1.5 to 43.5 nm, with an average size of ca. 7–10 nm. Nickel located on the nanofiber surface adopted a peculiar thin hexagonal morphology and almost no spheroidal particles were observed. From these results, it should be noted that depending on the nature of the metal, the morphology of the cluster could

vary or be modified during the drying and reduction steps over the carbon nanofiber support. The discrepancy between the present work and that of Baker and co-workers could be attributed to the difference between the nanofiber crystallinity which could influence the formation of the final metal morphology.

It is significant to note that after reduction some carbon nodules were observed on the nanofibers (Fig. 2). Such a phenomenon has never been reported in the literature and we have no clear explanation about its origin for the moment. It could possibly be due to an interaction between carbon and an intermediate of the exothermic decomposition of the nitrate counter ion or with the solvent used during the TEM preparation. However, similar catalytic results have been obtained on other forms of carbon nanostructure such as nanotubes which were exempt from such nodules which led us to conclude that they have no influence on the catalytic performance observed in the present work.

The catalyst surface area was slightly decreased from 50 to 45 m^2/g during the preparation. Such result could be attributed to some pore blockade of the support by palladium particles or to a slight modification of the carbon nanofibers during the reduction step in the presence of palladium catalyst at 400°C, i.e. carbon nodule formation as mentioned above. However, it was important to note that the palladium deposition did not create any microporosity in the material.

3.3. Hydrogenation of cinnamaldehyde in liquid-phase

Hydrogenation of cinnamaldehyde can be represented by the reaction pathway shown in Fig. 4. Cinnamaldehyde conversion and yield toward hydrogenated compounds obtained as a function of time on stream over the carbon nanofiber supported palladium catalyst, are presented in Fig. 5. At reaction temperatures up to 80°C, the C=C bond hydrogenation was exclusive (98%) whatever the conversion of cinnamaldehyde, and only traces of the corresponding saturated alcohol were detected in the reaction products (i.e. no unsaturated alcohol). It is generally well-known that palladium-based catalysts are efficient for the hydrogenation of the C=C double bond, but poor catalysts for the hydrogenation of aldehyde functions [44]. However, the use of palladium metal or a palladium complex usually leads

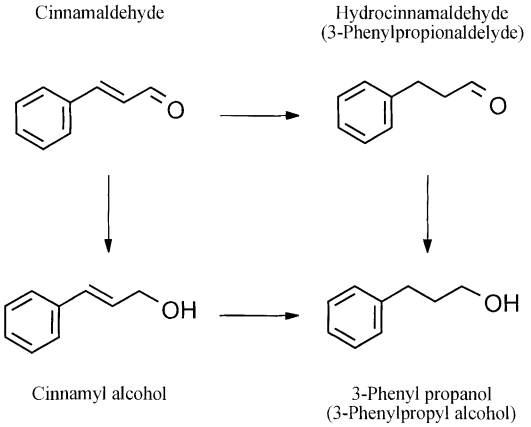

Fig. 4. Reaction pathway of the hydrogenation of cinnamaldehyde.

to a mixture of hydrocinnamaldehyde, cinnamyl alcohol and phenylpropanol [24,44]. Among various attempts to develop suitable palladium catalytic systems, it has been recently reported by Tin et al. [24] that palladium-complex-based catalysts could be efficiently employed to perform the selective hydrogenation of cinnamaldehyde into hydrocinnamaldehyde with an isolated yield of 91%. The C=O bond hydrogenation function of the catalyst was inhibited by the addition of Na_2CO_3 solution at pH 12.2.

For comparison, the catalytic test was also performed over the commercially available activated charcoal supported palladium catalyst (5 wt.% of palladium metal, supplied by Aldrich) under the same

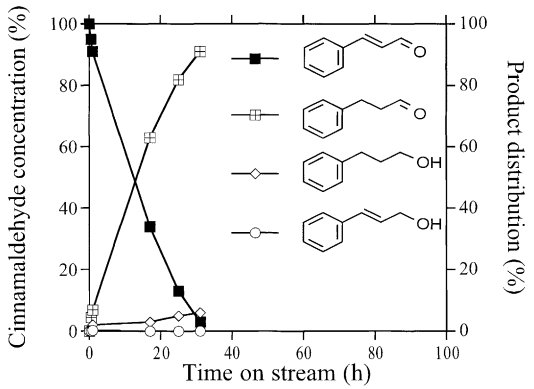

Fig. 5. Cinnamaldehyde conversion and product distribution as a function of time on stream obtained at 80°C over the carbon nanofiber supported palladium catalyst.

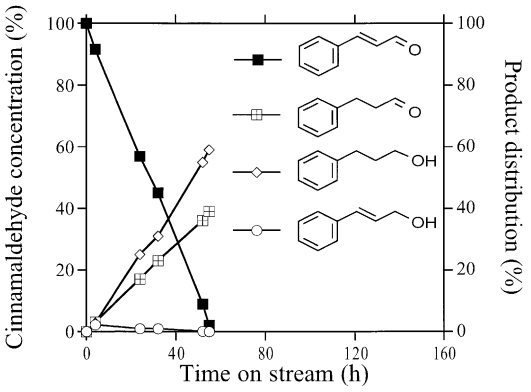

Fig. 6. Cinnamaldehyde conversion and product distribution as a function of time on stream obtained at 80°C over the commercially available activated charcoal supported palladium catalyst (5 wt.%).

reaction conditions. A mixture of saturated aldehyde and alcohol (corresponding to the hydrogenation of both C=C and C=O bonds) was detected whatever the conversion over the catalyst (Fig. 6).

Such results were in good agreement with those already published in the literature: Salman et al. [14] have reported that extensive hydrogenation was observed during the hydrogenation of crotonaldehyde over a graphite nanofiber supported nickel catalyst in a gas-phase reaction. Indeed, the extrastability of the C=O bond, conjugated via the C=C bond with the benzene ring in the cinnamaldehyde, was probably weakened after the hydrogenation of the C=C bond and may have been responsible for the non-selective reaction.

Our results show the superiority of the nanofiber-based catalyst (45 m^2/g) compared to the high surface area activated charcoal supported Pd (1000 m^2/g) for liquid-phase reactions. Such a phenomenon has already been reported by Baker et al., with nickel catalysts supported on graphite nanofibers and alumina [14]. High performances were quite surprising as the literature reported that a relatively low surface area creates a major drawback for such an application [3,6,14,41]. The high catalytic activity observed was attributed to the high external surface area (high surface-to-volume ratio) of the carbon nanofibers compared to the charcoal grains (grains size ca. 50–100 μm). The small diameter of the carbon nanofibers also allowed the decrease in the mass transfer phenomenon during the reaction which is predominant in liquid-phase reactions. In some cases, such a phenomenon can totally hinder the effectiveness of the catalyst itself. Furthermore, the presence of a large fraction of micropores (>60% of the total surface area) in the commercial catalyst can partially block the accessibility of the reactants to the palladium sites. The total absence of any microporosity in the nanofibers avoids such a drawback.

The higher degree of crystallinity of the carbon nanofibers compared to the activated charcoal could also explain the high activity obtained over the nanofiber-based catalyst. Rodriguez et al. have reported that Fe–Cu particles supported on graphite nanofibers exhibited a significantly higher activity for the conversion of hydrocarbons than when the same loading of bimetallic-phases was supported on either activated carbon or γ-alumina [45]. Studies performed by Chambers et al. showed that the performances of nickel particles supported on carbonaceous materials were extremely sensitive to the degree of crystalline perfection of the substrate, the highest hydrogenative activity being displayed by a system in which the metal was dispersed on nanofibers possessing a high graphitic content [13]. Such results were in close agreement with those reported earlier by Brownlie et al. using palladium decorated graphite catalysts [46]; the authors observed that the use of a well-ordered carbon support resulted in higher activities for the hydrogenation of selected hydrocarbons.

A peculiar metal–support interaction between the palladium metal crystallites and the support could also have an influence on product selectivity compared to the activated charcoal catalyst. Such an hypothesis has been proposed in the literature in order to explain specific selectivity obtained over nanofiber- or nanotube-based catalysts: strong improvements in the selectivity along with the use of nanostructures have been reported by Planeix and co-workers using ruthenium on various supports during the hydrogenation of cinnamaldehyde in liquid-phase [35,43] and by Salman et al. [14] during the hydrogenation of crotonaldehyde in a gas-phase. The hypothesis proposed by Baker and co-workers [13,47] involving a peculiar microstructure adopted by the palladium particles, which could allow selective adsorption of C=C bonds versus C=O bonds, should not be rejected.

The high selectivity obtained over the nanofiber-based catalyst could also be attributed to the absence of microporosity, generally very detrimental to the selectivity, by artificially increasing the contact time and also leading to successive hydrogenations. Indeed, the hydrocinnamaldehyde formed could be re-adsorbed in the microporosity of the activated charcoal support via the C=O bond, which was weakened after the C=C bond hydrogenation, thus, leading to the formation of the saturated alcohol. On the carbon nanofiber supported catalyst, the absence of microporosity favoured the rapid release of the primary reduction product from the catalyst surface into the liquid-phase. The re-adsorption of the hydrocinnamaldehyde was disadvantaged by competitive adsorption with (i) the starting product or (ii) the solvent itself. In addition, it should be stressed that the presence of some residual acidity on the activated charcoal surface could have favoured the hydrogenation of C=O bond in a consecutive reaction pathway [14,31].

4. Conclusion

Carbon nanofibers with a mean diameter centered at ca. 30–50 nm could be prepared by hydrocarbon decomposition over an alumina supported nickel catalyst with a relatively high yield and a gram-scale production. Palladium particles were homogeneously deposited on the outer surface of the carbon nanofibers by the classical incipient wetness impregnation method and displayed a spheroidal shape with a mean particle size centered at ca. 3–5 nm. The existence of a strong metal–support interaction between the metallic-phase and the graphite edges of the nanofibers was advanced to explain the observations. The use of carbon nanofibers as support resulted in a significant improvement in the cinnamaldehyde conversion rate in the liquid-phase reaction, compared to the commercially available palladium supported on activated charcoal. The high external surface area and the absence of any awkward microporosity in the Pd/CNF catalyst meant that the mass transfer limitation of the reactant to the active sites was inhibited and the apparent contact time of the products in the catalyst was diminished, leading to the obtention of an active and selective catalyst.

Acknowledgements

TEM experiments were performed at the Institut de Physique et Chimie des Matériaux de Strasbourg (IPCMS, UMR 7504 CNRS).

References

[1] S. Iijima, Nature (London) 354 (1991) 56.
[2] H. Fuchigami, A. Tsumura, H. Koezuka, Appl. Phys. Lett. 63 (1993) 1372.
[3] N.M. Rodriguez, J. Mater. Res. 8 (1993) 3233.
[4] N. Greenham, R. Friend, D. Bradley, Adv. Mater. 6 (1994) 491.
[5] J.P. Issi, L. Langer, J. Heremans, C.H. Olk, Carbon 33 (1995) 941.
[6] N.M. Rodriguez, A. Chambers, R.T.K. Baker, Langmuir 11 (1995) 3862.
[7] H. Dai, J.H. Hafner, A.G. Rinzler, D.T. Colbert, R.E. Smalley, Nature 384 (1996) 147.
[8] A. Fonseca, K. Hernadi, J.B. Nagy, D. Bernaerts, A.A. Lucas, J. Mol. Catal. A: Chem. 107 (1996) 159.
[9] A. Chambers, C. Park, R.T.K. Baker, N.M. Rodriguez, J. Phys. Chem. B 122 (1998) 4253.
[10] A. Peigney, Ch. Laurent, A. Rousset, J. Mater. Chem. 9 (1999) 1167.
[11] C. Liu, Y.Y. Fan, M. Liu, H.T. Cong, H.M. Cheng, M.S. Dresselhaus, Science 286 (1999) 1127.
[12] C. Park, R.T.K. Baker, J. Phys. Chem. B 102 (1998) 5168.
[13] A. Chambers, T. Nemes, N.M. Rodriguez, R.T.K. Baker, J. Phys. Chem. B 102 (1998) 2251.
[14] F. Salman, C. Park, R.T.K. Baker, Catal. Today 53 (1999) 385.
[15] P.N. Rylander, Catalytic Hydrogenation in Organic Syntheses, Academic Press, New York, 1979, p. 1.
[16] J.M. Smith, Chemical Engineering Kinetics, 3rd Edition, McGraw-Hill, New York, 1981, p. 450.
[17] R.J. Madon, M. Boudart, Ind. Eng. Chem. Fundam. 21 (1982) 438.
[18] S. Sato, R. Takahashi, T. Sodesawa, F. Nozaki, X.-Z. Jin, S. Suzuki, T. Nakayama, J. Catal. 191 (2000) 261.
[19] J.W. Geus, A.J. van Dillen, M.S. Hoogenraad, Mat. Res. Soc. Symp. Proc. 368 (1995) 87.
[20] F. Joo, A. Benyei, J. Organomet. Chem. 363 (1989) C19.
[21] J.M. Grosselin, C. Mercier, G. Allmang, F. Grass, Organomettalics 10 (1991) 2126.
[22] I.S. Cho, H. Alper, J. Mol. Catal. A: Chem. 106 (1996) 7.
[23] R. Sanchez-Delgado, M. Medina, F. Lopez-Linares, A. Fuentes, J. Mol. Catal. A: Chem. 116 (1997) 167.
[24] K.C. Tin, N.B. Wong, R.X. Li, J.Y. Hu, X.J. Li, J. Mol. Catal. A: Chem. 137 (1999) 121.
[25] H. Miura, M. Saito, J. Watanabe, K. Ichioka, T. Matsuda, Nippon Kagaku Kaishi 5 (1994) 489.
[26] Y. Nitta, K. Ueno, T. Imanaka, Appl. Catal. 56 (1989) 9.

[27] H. Nishiyama, T. Kubota, K. Kimura, S. Tsuruya, M. Masai, J. Mol. Catal. A: Chem. 120 (1997) L17.
[28] C. Ando, H. Kurokawa, H. Miura, Appl. Catal A: General 185 (1999) L181.
[29] M. Consonni, D. Jokic, D. Yu Murzin, R. Touroude, J. Catal. 188 (1999) 165.
[30] B. Heinrich, PhD Dissertation, Louis Pasteur University of Strasbourg, France, 1999.
[31] L. Zhang, J.M. Winterbottom, A.P. Boyes, S. Raymahasang, J. Chem. Technol. Biotechnol. 72 (1998) 264.
[32] S. Galvagno, A. Donato, G. Neri, R. Pietropaolo, D. Pietropaolo, J. Mol. Catal. A: Chem. 49 (1989) 223.
[33] S. Galvagno, G. Capannelli, G. Neri, A. Donato, R. Pietropaolo, J. Mol. Catal. A: Chem. 64 (1991) 237.
[34] S. Galvagno, A. Donato, G. Neri, R. Pietropaolo, G. Capannelli, J. Mol. Catal. A: Chem. 78 (1993) 227.
[35] B. Coq, P.S. Kumbhar, C. Moreau, P. Moreau, M.G. Warawdekar, J. Mol. Catal. A: Chem. 85 (1993) 215.
[36] H. Jaeger, T. Behrsing, Comp. Sci. Technol. 51 (1994) 231.
[37] Y. Ando, S. Iijima, Jpn. Appl. Phys 32 (1993) 107.
[38] V.P. Dravid, X. Lin, Y. Wang, A. Yee, J.B. Ketterson, R.P.H. Chang, Science 259 (1993) 1601.
[39] Y. Ando, Jpn. Appl. Phys 32 (1993) L1342.
[40] N. Hatta, K. Murata, Chem. Phys. Lett. 217 (1994) 398.
[41] M.-S. Kim, N.M. Rodriguez, R.T.K. Baker, Mat. Res. Soc. Symp. Proc. 368 (1995) 99.
[42] W. Teunissen, PhD Dissertation, University of Utrecht, The Netherlands, 2000.
[43] J.M. Planeix, N. Coustel, B. Coq, V. Brotons, P.S. Kumbhar, R. Dutartre, P. Geneste, P. Bernier, P.M. Ajayan, J. Am. Chem. Soc. 116 (1994) 7935.
[44] Y. Zhang, S. Liao, Y. Xu, D. Yu, Appl. Catal. A: General 192 (2000) 247.
[45] N.M. Rodriguez, M.S. Kim, R.T.K. Baker, J. Phys. Chem. 98 (1994) 13108.
[46] I.C. Brownlie, J.R. Fryer, G. Webb, J. Catal. 64 (1969) 263.
[47] R.T.K. Baker, K. Laubernds, A. Wootsch, Z. Paal, J. Catal. 193 (2000) 165.